An expanded non-Arrhenian model for silicate melt viscosity: A treatment for metaluminous, peraluminous and peralkaline liquids

D. Giordano [a,b,c,*], A. Mangiacapra [c,d], M. Potuzak [c], J.K. Russell [b], C. Romano [a], D.B. Dingwell [c], A. Di Muro [e]

[a] *Department of Geological Sciences, Third University of Rome, Largo Leonardo Murialdo 1, 00154 Rome, Italy*
[b] *Volcanology and Petrology Laboratory, Department of Earth and Ocean Sciences, University of British Columbia, Vancouver, Canada*
[c] *Department of Earth and Environmental Sciences, Munich University, Theresienstr. 41/III, 80333 Munich, Germany*
[d] *Istituto Nazionale di Geofisica e Vulcanologia-Osservatorio Vesuviano, Via Diocleziano 328, 80124 Napoli, Italy*
[e] *Laboratoire de Physique et Chimie des Systèmes Volcaniques, Paris VI-IPGP, 4 Place Jussieu, Paris, France*

Abstract

We present new viscosity measurements for melts spanning a wide range of anhydrous compositions including: rhyolite, trachyte, moldavite, andesite, latite, pantellerite, basalt and basanite. Micropenetration and concentric cylinder viscometry measurements cover a viscosity range of 10^{-1} to 10^{12} Pas and a temperature range from 700 to 1650 °C. These new measurements, combined with other published data, provide a high-quality database comprising ∼800 experimental data on 44 well-characterized melt compositions. This database is used to recalibrate the model proposed by Giordano and Dingwell [Giordano, D., Dingwell, D. B., 2003a. Non-Arrhenian multicomponent melt viscosity: a model. Earth Planet. Sci. Lett. 208, 337–349] for predicting the viscosity of natural silicate melts. The present contribution clearly shows that: (1) the viscosity (η)–temperature relationship of natural silicate liquids is very well represented by the VFT equation [$\log \eta = A + B/(T-C)$] over the full range of viscosity considered here, (2) the use of a constant high-T limiting value of melt viscosity (e.g., A) is fully consistent with the experimental data, (3) there are 3 different compositional suites (peralkaline, metaluminous and peraluminous) that exhibit different patterns in viscosity, (4) the viscosity of metaluminous liquids is well described by a simple mathematical expression involving the compositional parameter (SM) but the compositional dependence of viscosity for peralkaline and peraluminous melts is not fully controlled by SM. For these extreme compositions we refitted the model using a temperature-dependent parameter based on the excess of alkalies relative to alumina (e.g., AE/SM). The recalibrated model reproduces the entire database to within 5% relative error (e.g., RMSE of 0.45 logunits).
© 2006 Elsevier B.V. All rights reserved.

Keywords: Viscosity; Model; Silicate melts; Metaluminous; Peraluminous; Peralkaline

1. Introduction

The prediction of viscosity of silicate liquids, over the range of temperatures and compositions encountered in Nature, remains one of the most challenging and elusive goals in Earth Sciences. Recent work (Russell et

---

* Corresponding author. Department of Geological Sciences, Third University of Rome, Largo Leonardo Murialdo 1, 00154 Rome, Italy. Tel.: +39 050 8311929; fax: +39 050 8311942.
 E-mail address: dgiordan@uniroma3.it (D. Giordano).
 URL: http://www.giordano.pi.it (D. Giordano).

al., 2002, 2003; Giordano and Dingwell, 2003a; Russell and Giordano, 2005) suggests that there are now sufficient experimental measurements of melt viscosity to create new viscosity models to replace previous Arrhenian models (Shaw, 1972; Bottinga and Weill, 1972). The new data require that future viscosity models accommodate strong non-Arrhenian temperature dependencies (e.g., Richet, 1984; Hummel and Arndt, 1985; Angell, 1985) and extend the compositional range of more recent non-Arrhenian models (Hess and Dingwell, 1996).

Most recently, Giordano and Dingwell (2003a,b) presented an empirical model for accurately predicting the non-Arrhenian temperature-dependent viscosity and fragility of silicate melts over a wide range of anhydrous compositions (e.g., rhyolite to basanite). In this work, we extend their analysis to the widest range of anhydrous natural silicate melt compositions so far investigated. Our experimental database constitutes ~ 800 high quality measurements of viscosity on silicate melts that vary in character from strong to fragile (Angell, 1985). We use the purely empirical Vogel–Fulcher–Tamman (VFT) (Vogel, 1921; Fulcher, 1925; Tammann and Hesse, 1926) equation to accommodate the non-Arrhenian temperature dependence of melt viscosity (η):

$$\log \eta = A + B/(T-C) \qquad (1)$$

where η is the viscosity in Pa s and T is absolute temperature T (K). The variables A, B, and C are adjustable parameters representing the pre-exponential factor, the pseudo-activation energy, and the VFT-temperature, respectively (e.g., Angell, 1985). In this recalibration of the viscosity model we have also assumed that all silicate melts converge to a common value at high-temperature which requires that the value of A is constant and independent of composition (e.g., Russell et al., 2003; Russell and Giordano, 2005).

The database of experimentally determined pairs of values of T (K) vs. log η is substantially larger (about 800 data and 44 compositions) than originally available to Giordano and Dingwell (2003a) (about 800 data on 44 melt compositions vs. ~ 350 experiments on 20 different melt compositions). Also, the calibration provided here considers a temperature range from 613 to 2265 °C, much wider than that used by Giordano and Dingwell (2003a) (i.e., 700 to 1600 °C). Specifically, the new database comprises peralkaline (A.I. = ((Na$_2$O +K$_2$O)/Al$_2$O$_3$)>1), metaluminous and peraluminous (P.I. = Al$_2$O$_3$/CaO + Na$_2$O + K$_2$O>1) melt compositions. These data show that, compared to metaluminous liquids (Na$_2$O + K$_2$O < Al$_2$O$_3$ < CaO + Na$_2$O + K$_2$O), the

peralkaline and peraluminous melts have lower and higher viscosities, respectively.

Past and recent models of silicate melt viscosity have demonstrated the drastically different rheological behaviours of peralkaline, metaluminous and peraluminous melts. Multicomponent models based on the Arrhenian temperature dependence of viscosity (Shaw, 1972; Bottinga and Weill, 1972, Persikov, 1991) have shown that metaluminous melts typically have values of viscosity intermediate to those pertaining to peraluminous (higher viscosity) and peralkaline (lower viscosity) melts. The early models adopted an Arrhenian temperature dependence, fully consistent with the available data at the time, which is now viewed as inadequate as silicate melts commonly show a pronounced non-Arrhenian temperature dependence of viscosity (e.g., Angell, 1985; Richet and Bottinga, 1995; Dingwell, 1995; Giordano and Dingwell, 2003b; Russell et al., 2003). The seminal work from Bottinga and Weill (1972) and more recent studies that have incorporated both dry and H$_2$O-bearing melts (e.g., Baker and Vaillancourt, 1995; Dingwell et al., 1998a,b, 2000; Giordano et al., 2000; Whittington et al., 2000, 2001; Hess et al., 2001; Giordano and Dingwell, 2003a, b; Bouhifd et al., 2004; Webb et al., 2004) recognized that the rheological behaviour of peralkaline and peraluminous melts is complicated relative to metaluminous melts.

A simple recalibration of the Giordano and Dingwell (2003a) model using the extended database reproduces the viscosity data on metaluminous liquids very well but it is less accurate when predicting the viscosities of peralkaline and peraluminous melts at temperatures lower than 1000 °C. Lastly, we accommodate the discrepancies between the model predictions and the observed viscosities of peralkaline and peraluminous melts by an empirical factor based on the ratio of excess of alkalies over the alumina (AE = Na$_2$O + K$_2$O – Al$_2$O$_3$) to SM, the sum of all the structure modifier oxides. As defined in Giordano and Dingwell (2003a) SM is given by the sum on a molar basis of (Na$_2$O + K$_2$O + CaO + MgO + MnO + FeO$_{tot}$/2), disregarding for the contribution of charge-balancing cations. The temperature-dependent factor allows us to reproduce the complete database of melt viscosity to within a RMSE (Root Mean Square Error) of 0.45 logunits.

2. Experimental rationale

The quality, amount and distribution of experimental data strongly affect our ability to create new

predictive models. With this in mind we reduced the gaps in the T–X spaces, elucidated by Giordano and Dingwell (2003a), by measuring additional melt compositions (rhyolitic, trachytic, moldavitic, andesitic, latitic, pantelleritic, basaltic and basanitic) and incorporating them into the existing database of silicate melt viscosities from recent work (e.g., Neuville et al., 1993; Dingwell et al., 1996; Richet et al., 1996; Alibidirov et al., 1997; Whittington et al., 2000; Dingwell et al., 2000; Whittington et al., 2001; Giordano and Dingwell, 2003a; Bouhifd et al., 2004; Mangiacapra et al., 2005a,b; Giordano et al., submitted for publication). It is thanks to these new viscosity determinations and recent advances in modelling the viscosity of silicate melts (e.g., Russell et al., 2002, 2003; Giordano and Dingwell, 2003a) that we are now able to generalize previous observations to an extended database for multicomponent silicate systems.

The chemical composition and a description of the samples measured for this study are provided in Table 1 and Fig. 1. We also report the compositions of other natural and synthetic silicate melts for which viscosities have been measured by other research groups. The samples measured in this study correspond to natural samples collected in the field at different sites from the fallout deposits of the Fondo Riccio (Di Vito et al., 1999) (FRa) and the Campanian Ignimbrite (Civetta et al., 1997) (CI_OF*) plinian eruptions, at the Phlegrean Fields (PF, Italy). Other volcanic products were

collected at Stromboli (STB*) (Italy), Monserrat (MST) (Martinique), Slapany (SLP) (Czech Republic) and Merapi (MRP) (Indonesia) during their last phases of activity (see Table 1). They include a range of compositions from foidite and basanite to basaltic-andesites, andesites, phonolite, dacite and rhyolites (Fig. 1).

The starting materials used for the viscosity determinations were prepared by fusion of bulk rock samples. The experimental techniques used to measure the viscosity of the multicomponent liquid investigated include: (a) high-T (1050 to 1650 °C) concentric cylinder techniques for viscosity determinations in a range from about 10^{-1} to 10^5 Pa s, and (b) low-T micropenetration viscometry (676 to 919 °C) on quenched glasses to measure melt viscosity in the interval from about 10^8 to 10^{12} Pa s (e.g., near the glass transition temperature). Details of these experimental techniques have been described extensively in previous works (e.g., Dingwell and Virgo, 1988; Hess et al., 1995). The major element compositions of the glasses were determined using a Cameca SX 50 microprobe (Table 1).

The sets of measured values of viscosity are plotted in the Arrhenian diagram (Fig. 2). The complete data set used in this paper comprises that used by Giordano and Dingwell (2003a), as well as, the 144 new viscosity measurements on 8 new melt compositions reported in Table 2.

The database also uses viscosity determinations on multicomponent silicate melts reported by Neuville et al. (1993), Dingwell et al. (1996), Richet et al. (1996), Alibidirov et al. (1997), Toplis et al. (1997), Dingwell et al. (2000), Whittington et al. (2000, 2001), Bouhifd et al. (2004), Mangiacapra et al. (2005a,b), and Giordano et al. (submitted for publication). Over the temperature range of about 613 to 2265 °C, the measured compositions show near Arrhenian to strongly non-Arrhenian rheological behaviour.

3. Results and numerical strategy

As mentioned above, our new calibration adopts a slightly different strategy for modelling the viscosity of silicate melts as a function of temperature and composition with respect to the Giordano and Dingwell (2003a) model. Here we assume that all silicate liquids converge to a common, high-temperature limiting value of viscosity (e.g., Russell et al., 2002, 2003; Russell and Giordano, 2005). This assumption requires the parameter A to be constant and independent of melt composition (e.g., Angell, 1995). Consequently, all

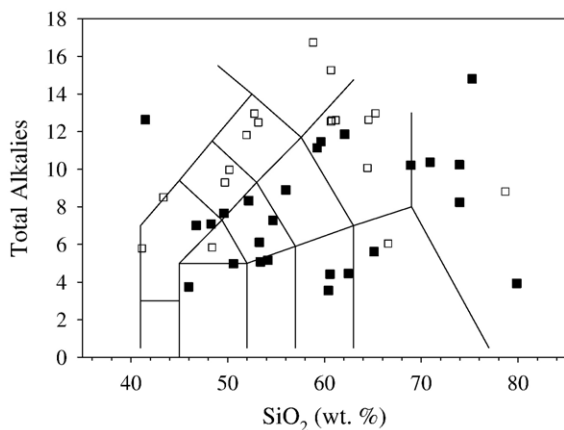Fig. 1. Chemical compositions of the (newly) investigated products (closed symbols) compared to compositions presented in Giordano and Dingwell (2003a) (G&D_'03) (open symbols). The chemical range of the samples investigated is given according to the T.A.S. (Total Alkali Silica) diagram (after Le Bas et al., 1986) reporting the values of the total alkali ($Na_2O + K_2O$) content vs. the SiO_2 (wt.%). Table 1 reports the chemical compositions as determined by microprobe analysis.

Table 1
List of samples used in this study including: rock type, sample label, composition (wt.% oxides) and reference source

Location	Sample	Composition	SiO$_2$	TiO$_2$	Al$_2$O$_3$	FeO$_{tot}$	MnO	MgO	CaO	Na$_2$O	K$_2$O	P$_2$O$_5$	SUM	SM	NBO/T	Ref.	
Nyiragongo (DRC)	NYI	Foidite	41.07	2.75	14.97	11.99	0.32	3.72	10.39	6.89	5.61	1.22	98.93	37.10	0.73	0	Scoria February 2002 eruption
Stromboli, I	STB*	Trachybas.	49.07	0.98	16.91	8.36	0.22	5.73	10.88	2.63	2.20	0.00	96.98	31.26	0.45	*	Scoria April 2003 eruption
Monserrat (Martiniq)	MST	Andesite	60.71	0.58	18.29	6.38	0.19	2.58	7.10	3.57	0.85	0.00	100.24	20.06	0.15	*	Tephra 1997 vulcanian eruption
PF, I	Min2a	Shoshonite	52.26	0.75	16.06	7.45	0.10	5.56	9.92	2.33	3.67	0.00	98.11	29.60	0.43	*	Tephra Minopoli eruption (10.3–9.5 ky) [10]
PF, I	Min2b	Shoshonite	53.72	0.64	17.47	7.22	0.17	3.78	8.07	3.63	3.53	0.00	98.23	26.11	0.30	*	Tephra Minopoli eruption (10.3–9.5 ky) [10]
PF, I	Fra	Latite	55.41	0.72	18.38	7.31	0.16	2.39	5.76	4.23	4.58	0.00	98.95	22.70	0.19	*	Tephra Fondo Riccio eruption (10.3–8 ky) [10]
PF, I	NYT*	Trachyte	58.77	0.50	18.39	4.96	0.06	1.43	4.03	3.38	7.67	0.00	99.18	19.16	0.12	*	Tephra Napoleitan Yellow Tuff eruption 15 ky [11]
PF, I	CL_OF*	Trachyte	68.80	0.23	12.58	3.17	0.14	1.24	3.43	4.01	6.18	0.03	99.84	16.20	0.16	*	Tephra Campanian Ignimbrite eruption 39 ky [12]
Slapany, CZ	SLP*	Basanite	45.76	2.27	12.52	11.30	0.25	11.42	11.45	2.65	1.07	0.86	99.55	39.57	0.90	*	Slapany Lava flow
Merapi (Indonesia)	MRP	Andesite	53.53	0.82	18.95	9.03	0.19	3.42	9.23	3.45	1.64	0.00	100.26	25.87	0.26	*	Tephra 1993 dome eruption
Moldavite	MDV	Moldavite	79.43	0.20	9.94	1.89	0.03	1.64	2.42	0.49	3.42	0.00	99.44	9.08	0.05	*	Tectite analogue
PF, I	IGC	Trachyte	60.74	0.27	19.22	3.37	0.18	0.28	2.11	5.28	6.32	0.06	97.83	15.58	0.04	1	
PF, I	MNV	Trachyte	63.88	0.31	17.10	2.90	0.13	0.24	1.82	5.67	6.82	0.05	98.93	15.35	0.07	1	
PF, I	AMS_B1	Trachyte	60.10	0.38	18.03	3.43	0.14	0.73	2.92	4.49	7.89	0.16	98.27	17.51	0.10	1	
PF, I	AMS_D1	Trachyte	59.98	0.39	18.01	3.82	0.11	0.88	2.91	4.06	8.37	0.21	98.75	17.75	0.11	1	
Vesuvius (I)	Ves_W	Phonolite	52.02	0.59	19.28	4.65	0.14	1.72	6.58	4.53	7.69	0.65	97.82	24.45	0.26	1	
Vesuvius (I)	Ves_G	Phonolite	51.24	0.58	19.14	4.55	0.12	1.71	6.51	4.60	7.99	0.71	97.14	24.80	0.28	1	
Montana Blanca (E)	Td_ph	Phonolite	60.46	0.56	18.81	3.31	0.20	0.36	0.67	9.76	5.45	0.06	99.64	17.88	0.10	1	
Unzen (Japan)	UNZ	Dacite	66.00	0.36	15.23	4.08	0.10	2.21	5.01	3.84	2.16	0.14	99.13	17.03	0.14	1	
Vesuvius, I	Ves_Gt	Phonoteph.	49.70	0.84	16.57	7.27	0.13	5.15	10.30	2.73	6.57	0.73	99.98	31.77	0.53	1	
Vesuvius, I	VesW_t	Tephriphon.	51.94	0.68	18.87	6.19	0.13	2.54	7.41	3.48	8.01	0.41	99.98	26.40	0.31	1	
Povocao, P	PVC	Trachyte	65.26	0.45	17.30	2.60	0.14	0.32	0.85	6.46	6.52	0.09	99.98	14.63	0.06	1	
Eifel, D	EIF	Basanite	41.14	2.74	12.10	10.11	0.18	11.24	15.66	2.76	3.04	1.02	99.98	44.71	1.17	1	
Etna, I	ETN	Trachybas.	47.03	1.61	16.28	10.13	0.20	5.17	10.47	3.75	1.94	0.59	97.18	32.04	0.51	1	
PF, I	ATN	Trachyte	60.66	0.47	18.82	3.66	0.17	0.66	2.85	3.95	8.59	0.15	99.98	17.15	0.09	1	
Mt Peleé (Martiniq)	ME1311e	Andesite	62.46	0.55	20.03	0.03	0.02	3.22	9.09	3.52	0.93	0.12	99.98	19.97	0.16	2	
Mt. St Helens (Wa.)	MSHD	Dacite	65.28	0.59	17.05	4.97	0.08	1.82	4.70	4.34	1.29	0.13	100.25	16.34	0.10	3	
	SiO$_2$		100	0.00	0.00	0.00	0.00	0.00	0.00	0.00	0.00	0.00	100.00	0.00	0.00	4	
	HPG8	Haplogran.	78.60	0.00	12.50	0.00	0.00	0.00	0.00	4.40	4.20	0.00	99.90	7.73	0.02	5	
	W_T	Trachytic	64.45	0.50	16.71	0.00	0.00	2.92	5.36	6.70	3.37	0.00	100.01	20.12	0.21	6a	
	W_ph	Phonolitic	58.82	0.79	19.42	0.00	0.00	1.87	2.35	9.31	7.44	0.00	100.00	21.27	0.19	6a	
	W_Tf	Tephritic	50.56	2.35	14.03	0.00	0.00	8.79	15.00	7.04	3.01	0.00	100.78	38.53	0.86	6b	
	NIQ	Basanitic	43.57	2.97	10.18	0.00	0.00	9.17	26.07	7.59	0.96	0.00	100.51	48.93	1.51	6b	
	N_An	Andesitic	62.40	0.55	20.01	0.00	0.02	3.22	9.08	3.52	0.93	0.12	99.88	19.97	0.16	7	
Stein Frentz, D	SFB	Tephritic	46.58	2.45	13.28	11.20	0.00	9.15	10.00	5.60	1.38	0.00	99.64	37.77	0.75	8	
Stein Frentz, D	SFB5	Tephritic	48.23	2.32	13.10	10.24	0.00	8.91	10.01	5.63	1.45	0.00	99.89	36.82	0.72	8	
Stein Frentz, D	SFB10	Phonoteph.	49.34	2.12	12.80	9.86	0.00	8.10	9.62	6.10	1.52	0.00	99.46	35.67	0.69	8	
Stein Frentz, D	SFB20	Mugearitic	51.58	1.51	12.12	8.94	0.00	7.24	9.24	5.44	1.76	0.00	98.87	34.14	0.66	8	
Stein Frentz, D	SFB40	Trachytic	58.97	1.58	9.86	7.24	0.00	4.56	5.33	8.99	2.34	0.00	98.87	27.71	0.50	8	
Stein Frentz, D	SFB60	Rhyolitic	74.84	0.50	4.24	1.20	0.00	1.98	1.96	11.34	3.39	0.00	99.45	19.41	0.40	8	
	HPG8An10	Synthetic	73.60	0.00	15.60	−1.00	0.00	0.00	2.10	4.40	3.80	0.00	98.50	9.42	−0.01	9	
	HPG8An20	Synthetic	71.50	0.00	17.30	0.00	0.00	0.00	4.00	4.20	3.50	0.00	100.50	11.54	0.01	9	
	HPG8An50	Synthetic	64.00	0.00	23.10	0.00	0.00	0.00	8.70	2.60	1.90	0.00	100.30	14.46	−0.01	9	
	HPG8An75	Synthetic	56.20	0.00	27.20	0.00	0.00	0.00	13.30	1.60	1.50	0.00	99.80	18.89	0.02	9	

0, Giordano et al. (submitted for publication); 1, Giordano and Dingwell (2003a); 2, Richet et al. (1996); 3, Alibidirov et al. (1997); 4, Toplis et al. (1997); 5, Dingwell et al. (1996); 6, Whittington et al. (2000, 2001); 7, Neuville et al. (1993); 8, Bouhifd et al. (2004); 9, Dingwell et al. (2000); 10, Di Vito et al. (1999); 11, Deino et al. (2004); 12, Civetta et al. (1997); *, this study.

Experimental conditions used during microprobe analysis are: 15 kV, 10 nA, spot 5 μm. The standard crystals and the counting time (in seconds) are as follows: TAP [Si (10); Al (10)]; LIF [Fe (20); Mn (60); Ti (60)]; PET [K (10)]; TAP [Na (10); Mg (10)].
Compositions were measured at the IPGP (Istitut du Globe Paris) using the conditions reported at the bottom of the table.
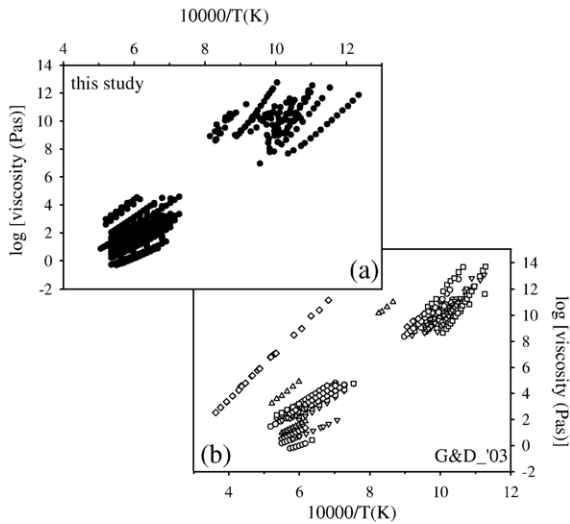
Fig. 2. (a) Viscosity data measured and analysed in this study (closed symbols) and (b) experimental data (open symbols) considered from Giordano and Dingwell (2003a) (G&D_'03). Data sets are reported in the viscosity-reciprocal temperature diagram, where viscosity is in logarithmic scale. Tables 1 and 2 report data sources and measured viscosity data for the silicate melts investigated.

compositional controls must be accommodated by variations in the B and C terms (Russell and Giordano, 2005). This assumption is also justified by theoretical studies (e.g., Glasstone et al., 1941; Myuller, 1955; Frenkel, 1959). Operationally, this is also justified because there is no statistical difference between the quality of fits of the VFT functions to individual data sets or to data sets coupled via a single optimized value of A (e.g., Russell et al., 2003; Russell and Giordano, 2005) (Fig. 3). The main consequence of this assumption is that the number of variables (e.g., A, B and C) necessary to describe the T-dependence of viscosity for N individual melt compositions is reduced from $3N$ (where N is the number of data sets) to $2N+1$.

For each melt composition we have calculated the optimum VFT coefficients (e.g., A, B and C). We have fit the individual data sets by first assuming that each has a different value of A and, then, by assuming they share a common, but unknown, value of A. The parameters obtained in the two different circumstances are reported in Table 3 with their respective χ^2 and the RMSE values. The results of the optimization are summarized in Fig. 3a and b where the misfits between calculated and measured values of viscosity are compared. For the individual fits the average is 0.24. In the case of a common value of the A parameter an optimal value of -4.07 (in logarithmic units) is found which agrees well with the pre-exponential factor ($A = 10^{-4.5 \pm 1}$ Pa s) predicted by theories based on kinetic rate processes

(e.g., Glasstone et al., 1941; Frenkel, 1959) and utilized by Myuller (1955) for the description of the Arrhenian T-dependence of viscosity. Furthermore, the resulting RMSE is 0.30 logunits, which is only slightly larger than the value of 0.24 logunits obtained for individual values of A (and $N-1$ extra parameters).

Given that A is constant and independent of composition, the compositional effects on melt viscosity must be completely accommodated by the values of B and C. The B and C parameters fitted with a constant value of A are strongly correlated and the covariation between the model values of B and C (Table 2) is illustrated in Fig. 4. The values of B and C parameters describe 3 separate trends for the metaluminous, peralkaline, and peraluminous melt compositions, respectively. Peralkaline melts tend to have lower values of C at fixed values of B, peraluminous have higher values of C and metaluminous are intermediate.

In particular, B and C values appear to be correlated with the degree of melt polymerisation expressed by the parameter SM (=Σ mol% (Na$_2$O +K$_2$O+CaO+MgO+MnO+FeO$_{tot}$/2) (Giordano and Dingwell, 2003a) (Fig. 5a, b). In fact, the values of B, taken separately for each compositional suite, decrease with the increasing of the SM parameter, whereas an opposite trend, even if a bit more scattered, is observed for the C parameter (Giordano and Dingwell, 2003b; Russell et al., 2003). At higher values of SM and increasing degree of depolymerisation (low B and high C values), the C values for the peralkaline and the metaluminous melts seem to merge. For peraluminous melt compositions the C parameter defines a different trend. In addition, at fixed values of SM the peralkaline "suite" typically shows lower C values with respect to both metaluminous and peraluminous melts. On the other hand, the peraluminous "suite" has the highest C and the lowest B values.

The SM parameter constitutes the dominant chemical control on B and C values. Nevertheless Figs. 4 and 5a and b illustrate that SM alone is not sufficient to describe the variations in B and C found for all melt compositions. In fact, the B and C parameters for melts ranging from peralkaline to peraluminous are poorly described by SM (Fig. 5a, b) suggesting that an additional compositional factor is required.

The anomalous behaviour of peralkaline and peraluminous liquids with respect to the B and C parameters is also evident in the patterns of isothermal viscosity vs. the SM parameter (Fig. 6a, b). At high temperatures (>1200 °C, Fig. 6a, b) and low values of viscosity (<10^5 Pa s, if pure silica is excluded) viscosity varies coherently as SM changes, regardless of whether

Table 2
Measured values of viscosity for individual melt compositions at specified temperatures

Sample name	T (°C)	log η (Pa s)	Sample name	T (°C)	log η (Pa s)	Sample name	T (°C)	log η (Pa s)
MST	1618.6	1.04	Fra	1421.7	1.72	SLP*	1323.2	0.45
MST	1593.9	1.11	Fra	1397.1	1.85	SLP*	1298.6	0.56
MST	1569.3	1.21	Fra	1372.5	1.97	SLP*	1274.0	0.68
MST	1544.7	1.32	Fra	1347.8	2.10	SLP*	1249.4	0.81
MST	1520.1	1.43	Fra	1323.2	2.24	SLP*	730.1	9.01
MST	1495.5	1.53	Fra	1298.6	2.38	SLP*	719.3	9.42
MST	1470.9	1.65	Fra	1274.0	2.52	SLP*	688.3	10.53
MST	1446.3	1.76	Fra	1249.4	2.67	SLP*	696.6	10.08
MST	1421.7	1.89	Fra	1224.8	2.83			
MST	1397.1	2.01	Fra	1200.2	2.99	MRP	1593.9	0.61
MST	1372.5	2.15	Fra	1175.6	3.16	MRP	1569.3	0.70
MST	1347.8	2.29	Fra	1151.0	3.35	MRP	1544.7	0.80
MST	1323.2	2.43	Fra	771.3	10.11	MRP	1520.1	0.89
MST	1298.6	2.58	Fra	765.7	10.05	MRP	1495.5	0.99
MST	1274.0	2.73	Fra	753.3	10.45	MRP	1470.9	1.09
MST	1249.4	2.90	Fra	749.1	10.52	MRP	1446.3	1.20
MST	1224.8	3.06	Fra	741.4	10.55	MRP	1421.7	1.31
MST	1200.2	3.25	Fra	734.0	10.65	MRP	1397.1	1.43
MST	753.4	9.74	Fra	713.7	10.99	MRP	1372.5	1.56
MST	739.6	10.18	Fra	711.9	10.98	MRP	1347.8	1.68
MST	688.7	11.60				MRP	1323.2	1.82
			CL_OF*	1593.9	2.02	MRP	1298.6	1.97
STB*	1593.9	0.21	CL_OF*	1569.3	2.14	MRP	1274.0	2.12
STB*	1569.3	0.28	CL_OF*	1544.7	2.26	MRP	1249.4	2.28
STB*	1544.7	0.37	CL_OF*	1520.1	2.39	MRP	1224.8	2.44
STB*	1520.1	0.45	CL_OF*	1495.5	2.52	MRP	1200.2	2.62
STB*	1495.5	0.54	CL_OF*	1470.9	2.66	MRP	1175.6	2.81
STB*	1470.9	0.64	CL_OF*	1446.3	2.80	MRP	1151.0	3.01
STB*	1446.3	0.74	CL_OF*	1421.7	2.94	MRP	1126.4	3.22
STB*	1421.7	0.84	CL_OF*	1397.1	3.10	MRP	722.9	10.5
STB*	1397.1	0.95	CL_OF*	1372.5	3.25	MRP	716.0	10.6
STB*	1372.5	1.06	CL_OF*	1347.8	3.42			
STB*	1347.8	1.16	CL_OF*	1323.2	3.59	MDV	1643.2	2.83
STB*	1323.2	1.29	CL_OF*	1298.6	3.76	MDV	1618.6	2.96
STB*	1298.6	1.42	CL_OF*	1274.0	3.94	MDV	1593.9	3.10
STB*	1274.0	1.56	CL_OF*	1249.4	4.13	MDV	1569.3	3.24
STB*	1249.4	1.70	CL_OF*	856.3	9.00	MDV	1544.7	3.38
STB*	1224.8	1.86	CL_OF*	836.3	9.31	MDV	1520.1	3.53
STB*	1200.2	2.02	CL_OF*	822.8	9.56	MDV	1495.5	3.69
STB*	1175.6	2.21	CL_OF*	797.2	10.08	MDV	1470.9	3.84
STB*	1151.0	2.39	CL_OF*	780.3	10.35	MDV	1446.3	4.01
STB*	729.5	9.35				MDV	1421.7	4.18
STB*	697.9	10.51	SLP*	1544.7	−0.31	MDV	1397.1	4.36
			SLP*	1520.1	−0.24	MDV	1372.5	4.53
Fra	1593.9	1.02	SLP*	1495.5	−0.19	MDV	919.6	9.43
Fra	1569.3	1.08	SLP*	1470.9	−0.12	MDV	882.3	10.11
Fra	1544.7	1.19	SLP*	1446.3	−0.03	MDV	864.7	10.45
Fra	1520.1	1.29	SLP*	1421.7	0.05	MDV	817.8	11.20
Fra	1495.5	1.40	SLP*	1397.1	0.15	MDV	954.7	8.92
Fra	1470.9	1.50	SLP*	1372.5	0.24			
Fra	1446.3	1.62	SLP*	1347.8	0.34			

the melts are metaluminous, peraluminous or peralkaline. The model isothermal viscosities at 1400 and 2000 °C are predicted simply as a function of the SM parameter. Even at 1000 °C there is a coherent trend between viscosity and

SM for most melts; the exceptions are two of the two peralkaline compositions (SFB40, SFB60), represented by the two squares with crosses under the 1000 °C isothermal viscosity curve in Fig. 6b. The discrepancies
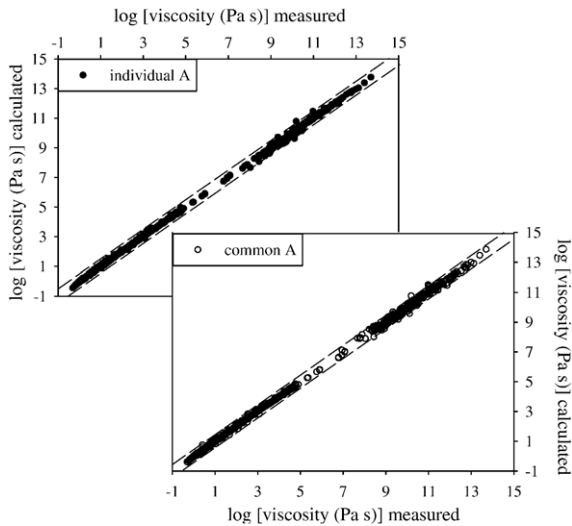
Fig. 3. Comparison between the measured values of viscosity (x-axis) and the values of viscosity predicted by fitting the data sets for individual melts to: (upper panel) independent values of A, B and C (Eq. (1)), and (lower panel) independent values of B and C coupled to a common value of A (=−4.07) for all the sets of data. VFT parameter and error analysis values are provided in Table 3. Parallel line indicates ±0.25 logunits.

between model isothermal viscosity curves and the measured values of viscosity increase as temperature decreases. The discrepancies are mainly related to the peralkaline and peraluminous liquids and they become substantial at temperatures below 800 °C (Fig. 6a, b). At these low temperature, the peralkaline samples show a viscosity significantly smaller than the metaluminous, whereas the peraluminous have higher viscosity compared to the metaluminous. According to these observations it seems reasonable to use the molar differences in alkali and alumina contents (AE=Na₂O+K₂O−Al₂O₃) as a useful chemical parameter to discriminate among the compositional suites. The reason for the above mentioned discrepancies is attributable to the different roles played in the silicate network by the structural arrangements provided by the network modifier and network former cations and in particular the mutual role played by the alkali and alumina.

Fig. 6 also shows that the isothermal curves become parallel at a critical amount of network modifiers (e.g., SM). The fact that the trends of the isothermal viscosity vs. the SM parameter are almost parallel indicate that they are also insensitive to temperature, possibly indicating that the effect of temperature on the structural rearrangement of silicate melts is probably quite limited. This is most apparent for melts having high values of SM values where the system is very depolymerised.

4. Viscosity model

Following the methods of Giordano and Dingwell (2003a), we have fitted empirical equations to the predicted values of viscosity for all melts at specific temperatures. For each melt composition (N=44) we computed the viscosity at a series of temperatures using a value of the A of −4.07 and the appropriate values of B and C (Table 3). Thus, for each specific temperature (see Fig. 6a) we computed 44 model values of viscosity corresponding to each of the different melt compositions represented by SM.

Isothermal curves were then generated by fitting equations of the form

$$\log_{10}\eta = a_1 + \frac{a_2 * a_3}{a_3 + \text{SM}} \qquad (2)$$

to the log η−SM data sets computed for each temperature. Thus, the isothermal variation in viscosity is described as a function of SM by the values of a_1, a_2, a_3 (Table 4). The present model uses a discrete number of isothermal viscosity curves at intervals of 100 °C over the range 700 °C to 2000 °C plus one at 630 °C. The temperature interval (630 to 2000 °C) investigated here is significantly larger than that used by Giordano and Dingwell (2003a).

Fig. 6a and b compares the values of viscosity (symbols) recalculated using the appropriate VFT functions at each temperature (630, 700, 800, 1000, 1400, and 2000 °C) to the model curves fitted to those data (curves) as a function of compositions (e.g., SM). The parameters (i.e., a_1, a_2, a_3) used for each isothermal viscosity curve are summarized in Table 4; these parameters allow melt viscosity to be predicted as a function of composition for specific temperatures. The values of these compositional parameters (e.g., a_1, a_2, a_3) vary with temperature (Fig. 7). Fig. 7 shows the values of these coefficients computed for discrete temperatures

$$a_1 = \frac{[-35.8816 + 0.0367110 \cdot T]}{[1 - 0.0022362 \cdot T - 0.00000166697 \cdot T^2]} \qquad (3)$$

$$a_2 = \frac{[-93.6494 + 0.2317411 \cdot T]}{[1 - 0.0054597 \cdot T + 0.00001361072 \cdot T^2]} \qquad (4)$$

$$a_3 = \frac{[-45.5755 - 0.0780935 \cdot T]}{[1 - 0.0036108 \cdot T - 0.00000002170 \cdot T^2]} \qquad (5)$$

which are represented by the curves (Eqs. (3)–(5)) in Fig. 7. In order to compute melt viscosity as a function of temperature and composition the following steps are taken: (i) compute the coefficients a_1, a_2, and a_3 for specified temperature using Eqs. (4)–(6); (ii) compute

Table 3
Model fits of VFT equation to individual data sets

Sample	N	Individual fit parameters					Common A parameters			
		Avft	Bvft	Cvft	χ^2	RMSE	Bvft	Cvft	χ^2	RMSE
SiO₂	26	−7.38	27,568.73	−24.48	0.07	0.05	16,110.07	421.44	0.45	0.13
IGC	18	−4.77	9184.30	473.71	0.12	0.08	7999.62	526.70	0.13	0.09
MNV	19	−6.05	13,653.62	165.01	0.02	0.03	9513.13	338.71	0.12	0.08
AMS_B1	11	−3.82	9055.89	362.24	0.07	0.08	9527.53	340.61	0.07	0.08
AMS_D1	14	−3.86	9107.49	350.21	0.09	0.08	9515.45	331.46	0.09	0.08
Ves_W	14	−6.76	12,183.32	265.80	0.09	0.08	7460.75	463.58	0.25	0.13
Ves_G	14	−6.34	11,559.47	304.76	0.35	0.16	7685.78	464.96	0.52	0.19
Td_ph	22	−4.94	11,068.55	220.81	0.02	0.03	9356.47	295.80	0.05	0.05
UNZ	20	−3.63	6878.87	545.14	0.02	0.03	7581.79	510.68	0.03	0.04
Ves_Gt	16	−4.98	6986.95	531.98	0.05	0.06	5591.25	601.23	0.10	0.08
VesW_t	12	−5.05	8069.69	467.16	0.03	0.05	6410.60	546.93	0.05	0.06
HPG8	10	−7.32	18,859.18	128.39	0.01	0.04	11,013.98	430.56	0.06	0.08
PVC	25	−5.68	13,003.54	205.44	0.04	0.04	9574.11	353.78	0.12	0.07
EIF	10	−4.24	4171.47	687.90	0.05	0.07	3958.80	699.35	0.05	0.07
ETN	10	−4.84	6019.41	602.37	0.03	0.06	4893.52	658.69	0.04	0.07
W_T	24	−3.61	7201.13	510.12	0.02	0.03	7957.46	474.82	0.06	0.05
W_ph	20	−3.22	7009.47	458.59	0.01	0.03	8372.12	396.59	0.14	0.08
W_Tf	22	−3.93	4662.72	639.99	0.08	0.06	4830.22	631.92	0.08	0.06
NIQ	20	−5.06	5289.38	605.55	0.02	0.03	4541.56	633.26	0.17	0.09
N_An	14	−3.97	7184.27	508.67	0.03	0.05	7355.36	500.77	0.03	0.05
ATN	17	−4.99	10,078.07	382.53	0.09	0.07	8428.82	456.38	0.11	0.08
MSHD	12	−5.08	10,008.47	372.45	0.02	0.04	8093.43	461.17	0.04	0.06
ME1311e	36	−4.36	7360.71	567.14	0.02	0.03	6905.56	588.03	0.05	0.04
NYI	23	−3.97	4257.07	677.48	0.34	0.12	4390.20	670.42	0.34	0.12
STB_B30	21	−3.70	4816.41	632.70	0.00	0.01	5331.53	605.24	0.02	0.03
MST	21	−4.25	7308.32	503.02	0.02	0.03	7021.19	516.73	0.02	0.03
Min_2a	25	−4.10	5749.19	584.80	0.16	0.08	5707.24	586.88	0.16	0.08
Min_2b	25	−3.66	5629.01	572.09	0.03	0.04	6237.55	541.20	0.06	0.05
FR_a	27	−4.66	7436.51	523.86	1.15	0.21	6530.46	566.17	1.20	0.21
NYT_lm*13*	24	−3.97	7390.22	514.10	0.02	0.03	7565.79	505.75	0.03	0.03
CL_OF104	20	−5.44	11,387.42	336.00	0.02	0.03	8683.52	457.97	0.07	0.06
Slapany	17	−4.44	4680.09	650.73	0.15	0.10	4209.57	675.93	0.17	0.10
MRP	22	−3.84	5636.13	600.77	0.01	0.02	5976.23	583.66	0.02	0.03
MDV_snt	17	−6.43	16,039.36	184.00	0.01	0.02	10,558.22	408.32	0.09	0.07
SFB	11	−3.47	3641.66	678.94	0.04	0.06	4380.17	638.49	0.05	0.07
SFB5	13	−3.56	4290.31	639.86	0.11	0.09	4856.70	612.16	0.18	0.12
SFB10	14	−4.50	5635.45	573.37	0.57	0.20	5114.99	598.16	0.60	0.21
SFB20	15	−3.41	4390.19	625.01	0.45	0.17	5138.79	587.84	0.56	0.19
SFB40	15	−3.15	5105.35	538.97	0.01	0.02	6318.20	479.64	0.18	0.11
SFB60	18	−1.82	4762.12	461.56	0.07	0.06	8206.66	282.26	0.96	0.23
HPG8An10	8	−6.20	15,552.56	221.44	0.01	0.03	10,576.73	428.68	0.02	0.05
HPG8An20	10	−4.37	10,213.29	456.98	0.00	0.00	9631.14	483.67	0.00	0.01
HPG8An50	12	−4.12	7235.99	636.87	0.02	0.05	7166.01	640.21	0.03	0.05
HPG8An75	14	−4.21	6076.60	727.36	0.04	0.05	5894.99	736.49	0.04	0.05

Model parameter values are reported for independent fits of each melt composition (A, B, C) and fits coupled by a common value of A (−4.07) and independent values of B and C. Also reported N, χ^2 and RMSE (root mean square error).

the value of SM for a specific melt composition, and (iii) compute the values of log η in Eq. (2) by using the model values of SM, a_1, a_2, and a_3.

Table 5 presents a sample calculation that shows how to compute the viscosity for a fixed temperature and composition.

Fig. 8 is a comparison of the experimentally measured values of the viscosity and the values predicted by the model represented by Eqs. (2)–(5). The model reproduces the viscosities of metaluminous liquids to an RMSE of 0.38 logunits. However, the model is less accurate in reproducing the viscosities of peraluminous and peralkaline compositions (Fig. 9b, c). Consequently, the RMSE value for the entire data set (e.g., 44 composition) is 0.84 logunits; calculations for the peraluminous and the peralkaline sample suites alone indicate RMSE values
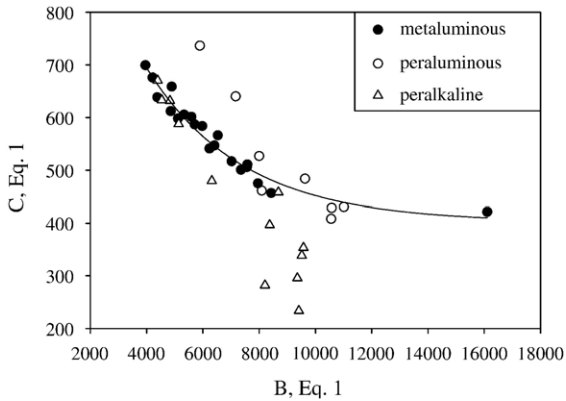
Fig. 4. Relationships between *B* and *C* for different compositional suites obtained from fitting all data simultaneously and assuming a constant value of *A*. Full circles, open circles and open triangles refer to metaluminous, peraluminous and peralkaline liquids, respectively.

of about 0.66 and 1.70, respectively. Nevertheless, these values are significantly lower than the RMSE values associated with the original Giordano and Dingwell
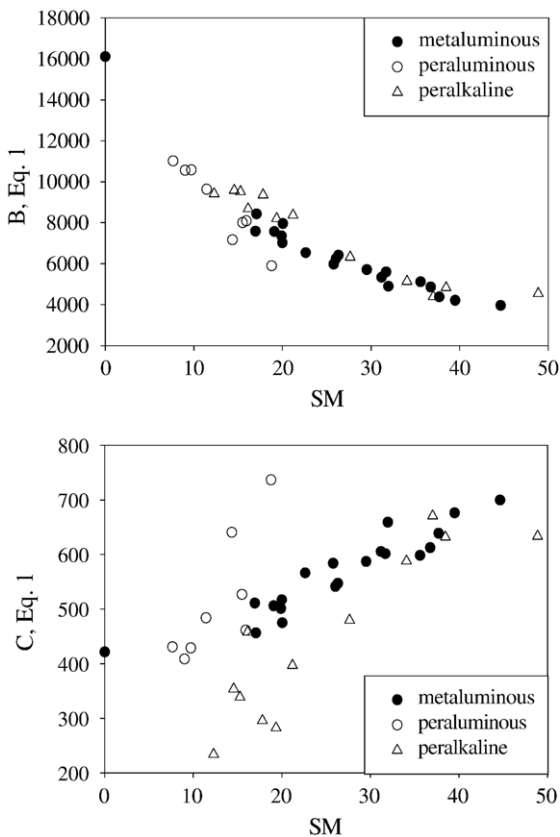

Fig. 5. Variation of the *B* and *C* parameters with the SM parameter (SM=Na_2O+K_2O+CaO+MgO+MnO+FeO_{tot}/2 (mol%); Giordano and Dingwell, 2003a). To a first approximation SM represents the "polymerisation degree" of the silicate network. Symbols as in Fig. 3.
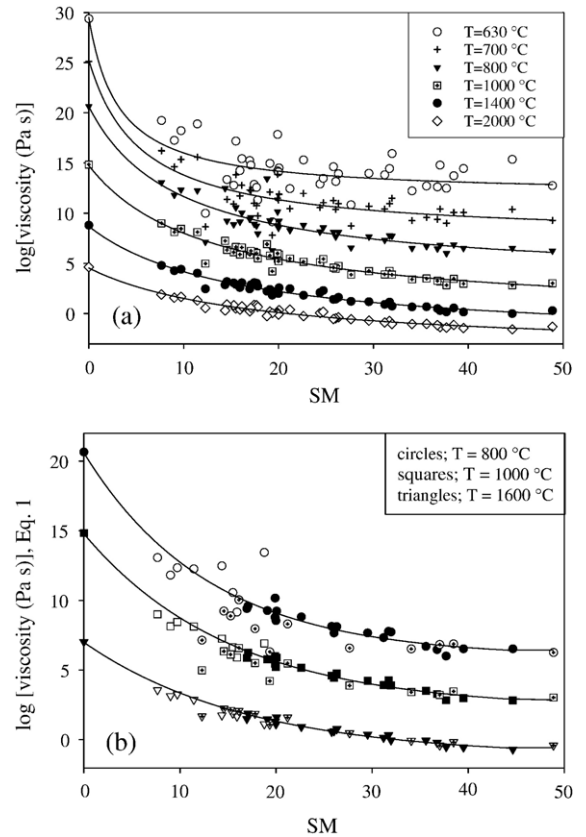
Fig. 6. (a) Isothermal viscosity at six different temperatures (630, 700, 800, 1000, 1400, 2000 °C) vs. the SM parameter. Numbers in the legend are temperatures (°C). Symbol positions are calculated from composition (SM) and from Eq. (1) using ideal values of *B*, *C* and *A*= −4.07. (b) Circles, squares and triangles correspond to a detail of the 800, 1000 and 1600 isothermal curves, respectively. Symbols are also differentiated to show metaluminous (filled), peraluminous (open), and peralkaline (crossed) melt compositions.

(2003a) model; suggesting that this current model represents a real and substantial improvement.

5. Extension to peralkaline and peraluminous melts

In order for this model to have wide application to natural systems, it is critical to find a means of capturing the behaviour of and accurately predicting viscosity for peraluminous and peralkaline melts. Fig. 9 shows the misfit of the current model (Eqs. (2)–(6)) to the measured values of viscosity for metaluminous, peralkaline and peraluminous melts as a function of the experimental reciprocal temperature. From examining Fig. 9 we can observe the following critical phenomena: (1) the model overestimates the viscosity of peralkaline melts (negative value of the residuals), (2) the model underestimates the viscosity of peraluminous (positive value

Table 4
Isothermal viscosity curve values for the a_i coefficients of Eq. (2)

T (°C)	a_1	a_2	a_3
630	11.7979	17.715	3.116
670	9.15816	17.813	4.507
700	7.54986	17.731	5.450
800	3.3433	17.288	9.2741
900	1.1136	16.185	11.020
1000	−0.3258	15.078	12.378
1100	−1.2886	14.039	13.423
1200	−1.9651	13.099	14.269
1300	−2.4516	12.258	14.936
1400	−2.8139	11.508	15.491
1500	−3.0908	10.828	15.998
1600	−3.3099	10.231	16.432
1800	−3.6018	9.1890	17.058
2000	−3.8001	8.3428	17.587

of the residuals), (3) the largest residuals are associated with peralkaline liquids, (4) metaluminous melts have very small random residuals and (5) the residuals are temperature-dependent and their absolute values increase with decreasing temperature. Along with these observations we believe that the observed discrepancies are strongly governed by the relationships between alkali and alumina. In particular, as discussed below, the discrepancies relate to the alkali excess over the alumina content (AE) and the network modifiers content.

Fig. 9 constitutes a first step in our analysis and provides a guide towards the form of equation that could be used to modify the current model and ensure that it also reproduces the viscosities of peraluminous and peralkaline melts. For example, on the basis of Fig. 9 we noticed that the magnitude of the misfit between model and data increases as a function of (i) increasing excess of alkali (AE) and (ii) decreasing SM values. Our goal at this point (see below) is to refine the model represented by Eqs. (2)–(6) so that it can be extended in a "continuous" way to reproduce all of the experimental data. We have adopted a simple temperature-dependent parabolic equation to describe the residuals for the peralkaline and peraluminous melts as a function of composition. Compositional variation is treated as different amounts of excess alkali (AE) and the number of structural modifiers (SM). The equation has the form:

$$\Delta \log \eta = \log \eta_{\text{meas}} - \log \eta_{\text{SM-model}}$$
$$= -0.000012923 \cdot T^2 \cdot \left(\frac{\text{AE}}{\text{SM}}\right)$$
$$+ 0.03578 \cdot T \cdot \left(\frac{\text{AE}}{\text{SM}}\right) - 24.337 \cdot \left(\frac{\text{AE}}{\text{SM}}\right) \quad (6)$$

where $\log \eta_{\text{meas}}$ is the measured value of viscosity, $\log \eta_{\text{SM-model}}$ is the viscosity predicted by Eqs. (2)–(5), T is

the temperature in Celsius; AE is the excess of alkalies over the alumina (AE = $Na_2O + K_2O - Al_2O_3$) and SM is the "structure modifier" parameter as defined by Giordano and Dingwell (2003a). The resulting parabolic equation provides a T-dependent correction factor as a function of the ratio AE/SM which can be added to Eq. (4) (see Eq. (7) below). As previously described Eqs. (2)–(5) were calibrated against parameters derived for a discrete number of isothermal viscosity ($\log \eta$) vs. SM curves (i.e., Table 4) over the temperature interval (630–2400 °C). This temperature interval was chosen because for most of the compositions analysed over that interval there is still a sufficient number of experimental data. At lower temperature only few composition were measured.

Our final regression of the experimental data for the model parameters is performed on the experimental
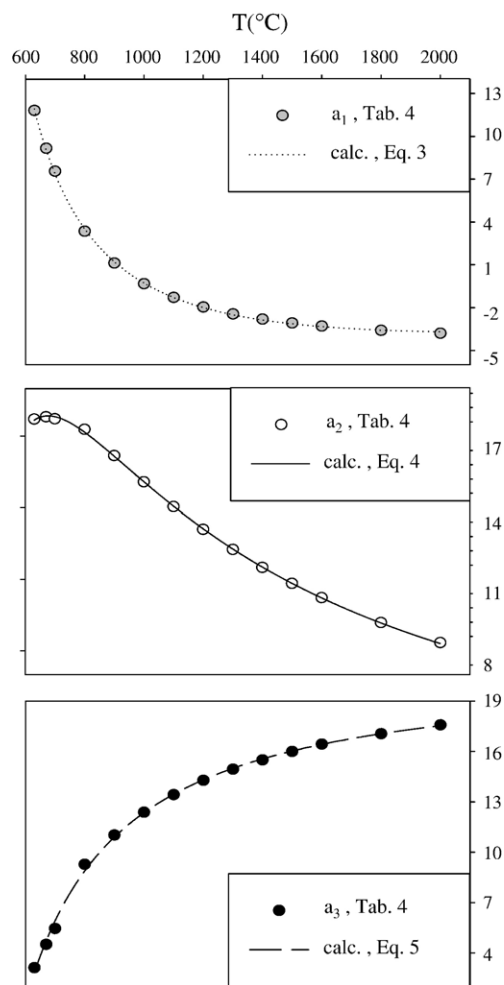

Fig. 7. Temperature dependence of the a_1, a_2, and a_3 parameters obtained by fitting isothermal viscosity values (Fig. 6). Curves in the figures correspond to (a) Eq. (3); (b) Eq. (4); (c) Eq. (5).

Table 5
Example of viscosity calculation for the Campanian Ignimbrite sample (IGC) at 1200 °C

Sample name (IGC)	Input values Composition (wt.%)	Output values Composition (mol%)		Calculated parameters (Eqs. (8)–(11))	
SiO_2	60.74	70.31			
TiO_2	0.27	0.24	b_1	−2.115425225	
Al_2O3	19.22	13.11	b_2	13.12945529	
Fe_2O_3 [a]	1.69	0.73	b_3	14.30849252	
FeO [a]	1.69	1.63	b_4	0.002671818	
MgO	0.28	0.48			
CaO	2.11	2.62	$\log \eta$ (Pa s)	4.173	
Na_2O	5.28	5.93			
K_2O	6.32	4.67			
P_2O_5	0.06	0.03			
MnO	0.18	0.18			
H_2O [b]	0.02	0.08			
Sum	97.83	100.00			

FeO_{tot} [a]	3.37	Molar amount	Model coefficients			
			Eq. (8)	Eq. (9)	Eq. (10)	Eq. (11)
SM		15.58	−33.5556	0.03516228	−0.0022362	−1.66697E-06
AE		−2.52	−93.6494	0.2317411	−0.0054597	1.36107E-05
AE/SM		−0.1618	45.575455	−0.0780935	−0.0036108	−2.17E-08
T (°C)	1200		−1.29239E-05	0.03577545	−24.3366274	

Inputs are the temperature in degree Celsius and the composition in wt.%.

[a] FeO and Fe_2O_3 are arbitrarily calculated assuming that half of the total iron FeO_{tot} (wt.%) is treated as FeO and the remaining half is treated as Fe_2O_3.

[b] According to the observations from Ohlhorst et al. (2001), that a residual amount of water is always present also in remelted liquid, we have added a fixed amount of water of 200 ppm to the chemical analysis for "virtually dry" samples.

database, rather than on discrete model values (e.g., Fig. 10 and Table 2). The resulting model is given by the equation:

$$\log_{10}\eta = b_1 + \frac{b_2 * b_3}{b_3 + SM} + b_4 \qquad (7)$$

where

$$b_1 = \frac{[-33.5556 + 0.0351623 \cdot T]}{[1 - 0.0022362 \cdot T - 0.00000166697 \cdot T^2]} \qquad (8)$$

$$b_2 = \frac{[-93.6494 + 0.2317411 \cdot T]}{[1 - 0.0054597 \cdot T + 0.00001361072 \cdot T^2]} \qquad (9)$$

$$b_3 = \frac{[45.575455 - 0.0780935 \cdot T]}{[1 - 0.0036108 \cdot T - 0.00000002170 \cdot T^2]} \qquad (10)$$

$$b_4 = -0.00001292391 \cdot \left(\frac{AE}{SM}\right)$$
$$\cdot T^2 + 0.03577545 \cdot \left(\frac{AE}{SM}\right)$$
$$\cdot T - 24.3366274 \cdot \left(\frac{AE}{SM}\right) \qquad (11)$$

T (°C) being the temperature in degree Celsius and the AE and SM are as defined above.

Eq. (11) comprises 15 empirical parameters which reproduce the entire database of viscosity measurements, including peralkaline and peraluminous samples, very well (Fig. 10)). The resulting fit has RMSE=0.45 logunits. Fig. 11 shows residuals as a function of SM. The largest differences between observed and model viscosity (Eqs. (7)–(11)) are in the peralkaline melts.

6. Discussion

It is clear that metaluminous, peraluminous and peralkaline melts analysed in this work define three different domains/regimes of viscous flow. At constant T, the metaluminous melts are more viscous than the peralkaline and less viscous than the peraluminous. It is also clear that such differences are determined by how the alumina and the alkali enter the structure of silicate melts. In particular, as discussed by Dingwell et al. (1998a,b), the viscosity for the haplogranitic composition (HPG8) increases with the addition of the first few percent of normative corundum, whereas it remains constant with further addition of Al_2O_3 (up to 5 wt.%).
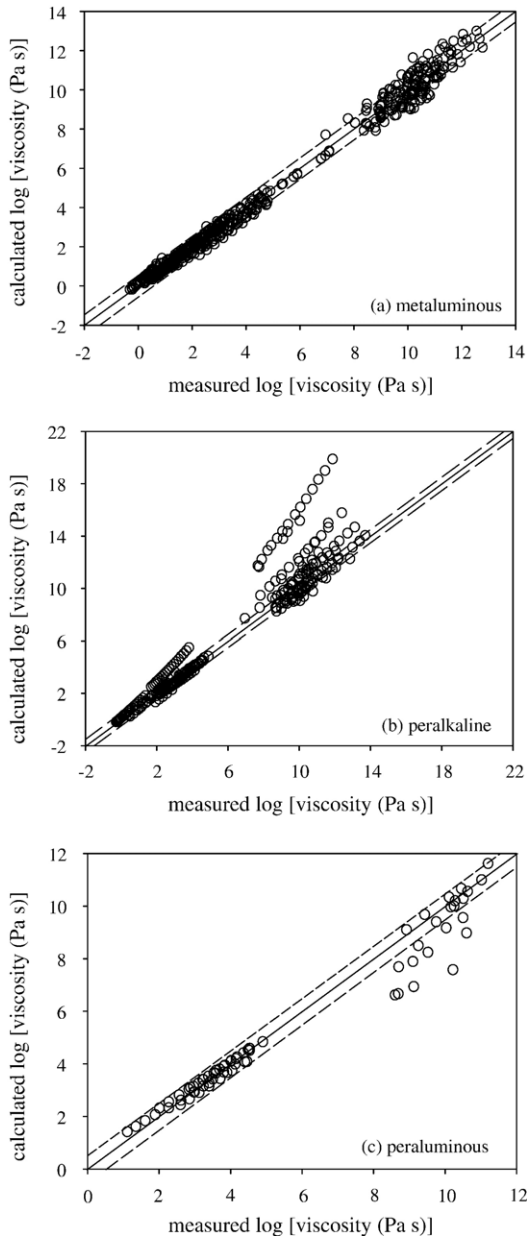
Fig. 8. Predicted vs. measured viscosity calculated by Eqs. (2)–(5). (a) Metaluminous; (b) peralkaline; (c) peraluminous liquids.

tigating the tricluster hypothesis in more detail. In contrast to what was observed by Toplis et al. (1997) for simple systems, we find that peralkaline melts show a more complex relationship between viscosity and chemical composition. The viscosity maximum is not shifted to the peralkaline field and the decrease in viscosity with addition of alkali is more pronounced than what is expected by a simple depolymerisation
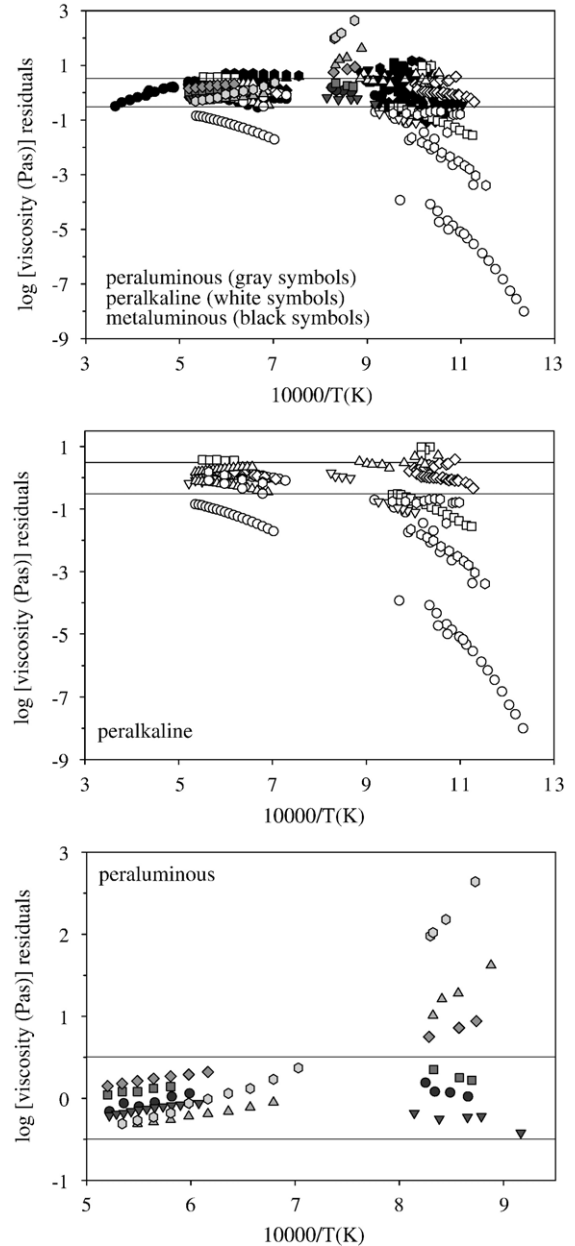
Fig. 9. Temperature dependence of the differences between viscosity calculated using Eqs. (2)–(5) and the measured values. Lines in the figure constrain the 2σ error interval.

A smooth variation of viscosity, in this compositional range, would require a viscosity maximum for a slightly peraluminous melt (between HPG8Al02 and HPG8Al05). Such a maximum, shifted with respect to the metaluminous composition, was also found along a stoichiometrically similar join in the system $Na_2O–Al_2O_3–SiO_2$ and was accounted for by the presence of triclusters in the melt (Toplis et al., 1997).

Unfortunately, the lack of viscosity data on strongly peraluminous melts prevents us from inves-

Fig. 10. Comparison of viscosity calculated by Eqs. (2)–(7) to measured viscosity. The total RMSE value is 0.45 logunits.

process as defined by either the SM (Giordano and Dingwell, 2003a) or the NBO/T parameter (Mysen et al., 1988). This decrease in viscosity correlates to the ratio AE/SM.

As already argued by Giordano and Dingwell (2003a,b), an explanation for this anomalous behaviour might be worth seeking in the notion of percolation channels in silicate melts affecting their medium-range order: a notion arising from experimental studies (e.g., Brown et al., 1995; Greaves and Ngai, 1995; Poggemann et al., 2003) and supported by molecular dynamics simulations (e.g., Horbach et al., 2001; Meyer et al., 2002). It is possible that, for strongly peralkaline melts, the depolymerisation of the structure is accompanied by modifications in the configurations of the percolation channels leading to changes in the viscous regime of these melts. Additional data on strongly peraluminous natural melts and strongly peralkaline natural melts are necessary in order to further explore these interpretations.

7. Summary and conclusion

On the basis of an extended database comprising the viscosity of natural multicomponent silicate melts and recent viscosity determination from other research group we have analysed the T-variation of the viscous response of strong and fragile liquids within a wide range of compositions and identified three well distinguished compositional suites (i.e., peralkaline, metaluminous and peraluminous) showing a clear contrast in their viscosity. We presented an extended model to calculate the viscosity of silicate melts over a wide range of temperatures and compositions. This model constitutes a significant improvement with
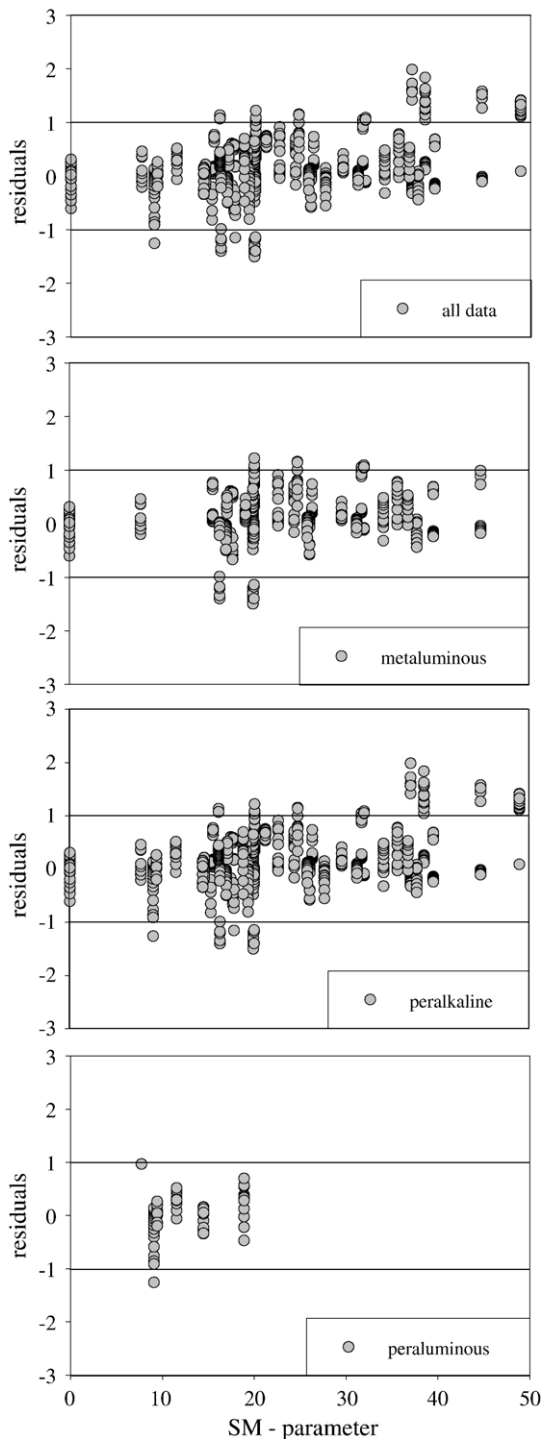

Fig. 11. Residual viscosity values calculated according to Eqs. (7)–(11) vs. the SM parameter. Figures refer to all data together and separately for metaluminous, peralkaline and peraluminous melts. Figure shows that residuals increase towards higher values of the SM parameter. Lines in the figures constrain the 2σ interval.

respect to the Giordano and Dingwell (2003a) study in that: (1) the number of experimental determinations over which the model is calibrated is larger; (2) the range of investigated compositions is larger; (3) the investigated temperature range is larger; (4) the assumption is made that at infinite temperature, the viscosity of silicate melts converges to a common, but unknown value of the pre-exponential factor ($A=-4.07$, Eq. (1)). In particular the compositional range involves a large number of viscosity determinations for peralkaline and peraluminous compositions in a temperature interval between 676 and 2380 °C. Furthermore, it has been shown that the assumption of a common value of the pre-exponential parameter A produces an equally good representation of the experimental data as would allowing each melt to have individual values of A. This optimization also induces a strong coupling between data sets that stabilizes the range of solutions and allows to discriminate between the different rheological behaviour of extreme compositions (peralkaline and peraluminous vs. metaluminous).

We demonstrated that, although the parameter SM (Giordano and Dingwell, 2003a) can be used to model compositional controls on the viscosities of metaluminous liquids, it does not capture the viscosity of peralkaline and peraluminous liquids. The differences in the rheological behaviour of these extreme compositions reflect important differences in the structural configuration of metaluminous, peralkaline and peraluminous melts. Subsequently we performed a second regression of the experimental data involving a second compositional parameter (AE) that accounts for the excess of alkali oxides over the alumina. Incorporating this temperature-dependent compositional parameter (i.e., AE) into the SM-based model (Eq. (7)) appears to account for the anomalous rheological behaviour of peralkaline and peraluminous liquids. The resulting model reproduces the entire experimental database to within and average RMSE of 0.45 logunits. We recommend use of the present model for estimation of the viscosity of anhydrous multicomponent silicate melts of volcanic interest.

Acknowledgements

References

Alibidirov, N., Dingwell, D.B., Stevenson, R.J., Hess, K.-U., Webb, S. L., Zinke, J., 1997. Physical properties of the 1980 Mount St. Helens cryptodome magma. Bull. Volcanol. 59, 103–111.

Angell, C.A., 1985. Strong and fragile liquids. In: Ngai, K.L., Wright, G.B. (Eds.), Relaxations in Complex Systems. U.S. Department of Commerce National Technical Information Service, Springfield, VA, pp. 3–11.

Angell, C.A., 1995. Formation of glasses from liquids and byopolymers. Science 265, 1924–1935.

Baker, D.R., Vaillancourt, J., 1995. The low viscosities of F+H_2O-bearing granitic melts and implications for melt extraction and transport. Earth Planet. Sci. Lett. 132, 199–211.

Bottinga, Y., Weill, D., 1972. The viscosity of magmatic silicate liquids: a model for calculation. Am. J. Sci. 272, 438–475.

Bouhifd, A.M., Richet, P., Besson, P., Roskosz, M., Ingrin, J., 2004. Redox state, microstructure and viscosity of a partially crystallized basalt melt. Earth Planet. Sci. Lett. 218, 31–44.

Brown, G.E., Farges, F., Calas, G., 1995. X-ray scattering and X-ray spectroscopy studies of silicate melts. Rev. Mineral. 32, 317–410.

Civetta, L., Orsi, G., Pappalardo, L., Fisher, R.V., Haiken, G., Ort, M., 1997. Geochemical zoning, mingling, eruptive dynamics and depositional process. The Campanian Ignimbrite, Campi Flegrei caldera, Italy. J. Volcanol. Geotherm. Res. 75, 183–219.

Deino, A.L., Orsi, G., Piochi, M., de Vita, S., 2004. The age of the Neapolitan Yellow Tuff caldera-forming eruption Campi Flegrei caldera–Italy. Assessed by 40Ar/39Ar dating method. J. Volcanol. Geotherm. Res. 133, 157–170.

Dingwell, D.B., 1995. Relaxation in silicate melts: applications. In: Stebbins, J., McMillan, P.F., Dingwell, D.B. (Eds.), Structure, Dynamics and Properties of Silicate Melts. Reviews in Mineralogy, vol. 32. Mineralogical Society of America, Washington, DC, pp. 21–66.

Dingwell, D.B., Virgo, D., 1988. Melt viscosities in the Na_2O–FeO–Fe_2O_3–SiO_2 system and factors controlling the relative viscosities of fully polymerised silicate melts. Geochim. Cosmochim. Acta 52, 395–403.

Dingwell, D.B., Romano, C., Hess, K.U., 1996. The effect of water on the viscosity of a haplogranitic melt under P-T-X-conditions relevant to silicic volcanism. Contrib. Mineral. Petrol. 124, 19–28.

Dingwell, D.B., Hess, K.U., Romano, C., 1998a. Viscosity data for hydrous peraluminous granitic melts: comparison with a metaluminous model. Am. Mineral. 83, 236–239.

Dingwell, D.B., Hess, K.U., Romano, C., 1998b. Extremely fluid behaviour of hydrous peralkaline rhyolites. Earth Planet. Sci. Lett. 158, 31–38.

Dingwell, D.B., Hess, K.U., Romano, C., 2000. Viscosities of granitic sensu lato.: influence of the anorthite component. Am. Mineral. 85, 1342–1348.

Di Vito, M.M., Isaia, R., Orsi, G., Southon, J., de Vita, S., D'Antonio, M., et al., 1999. Volcanism and deformation since 12,000 years at the Campi Flegrei caldera Italy. J. Volcanol. Geotherm. Res. 91, 221–246.

Frenkel, Y.I., 1959. The Kinetic Theory of Liquids. Selected Works, vol. 3. Izd. Akad. Nauk SSSR, Moscow (in Russian).

Fulcher, G.S., 1925. Analysis of recent measurements of the viscosity of glasses. J. Am. Ceram. Soc. 8, 339–355.

Giordano, D., Dingwell, D.B., 2003a. Non-Arrhenian multicomponent melt viscosity: a model. Earth Planet. Sci. Lett. 208, 337–349.

Giordano, D., Dingwell, D.B., 2003b. The kinetic fragility of natural silicate liquids. J. Phys., Condens. Matter 15, S945–S954.

Giordano, D., Dingwell, D.B., Romano, C., 2000. Viscosity of a Teide phonolite in the welding interval. J. Volcanol. Geotherm. Res. 103, 239–245.

Giordano, D., Polacci, M., Dingwell, D.B., Papale, P., Kasereka, M., Potuzak, M., et al., submitted for publication. Textural and rheological constraints on the dynamics of the January 17th, 2002 fissure eruption at Mount Nyiragongo. Geophys. Res. Lett.

Glasstone, S., Laidler, K., Eyring, H., 1941. Theory of Rate Processes. McGraw-Hills, New York.

Greaves, G.N., Ngai, K.L., 1995. Reconciling ionic-transport properties with atomic structure in oxide glasses. Phys. Rev., B 52, 6358–6380.

Hess, K.U., Dingwell, D.B., 1996. Viscosities of hydrous leucogranitic melts: a non-Arrhenian model. Am. Mineral. 81, 1297–1300.

Hess, K.U., Dingwell, D.B., Webb, S.L., 1995. The influence of excess alkalis on the viscosity of a haplogranitic melt. Am. Mineral. 80, 297–304.

Hess, K.U., Dingwell, D.B., Gennaro, C., Mincione, V., 2001. Viscosity-temperature behaviour of dry melts in the Qz–Ab–Or system. Chem. Geol. 174, 133–142.

Horbach, J., Kob, W., Binder, K., 2001. Structural and dynamical properties of sodium silicate melts: an investigation by molecular dynamics computer simulation. Chem. Geol. 174, 87–102.

Hummel, W., Arndt, J., 1985. Variation of viscosity with temperature and composition in the plagioclase system. Contrib. Mineral. Petrol. 90, 83–92.

Le Bas, M.J., Le Maitre, R.W., Streckeisen, A., Zanetti, R., 1986. A chemical classification of volcanic rocks based on the total-alkali-silica diagram. J. Petrol. 27, 745–750.

Mangiacapra, A., Giordano, D., Potuzak, Dingwell, D.B., 2005. Modelling Non-Arrhenian Multicomponent Melt Viscosity: The Effect of the Iron Oxidation State in Progress.

Mangiacapra, A., Di Matteo, V., Giordano, D., Nichols, A.R.L., Dingwell, D.B., Orsi, G., 2005. Water and the Viscosity of Shoshonitic and Latitic Melts in Progress.

Meyer, A., Schober, H., Dingwell, D.B., 2002. Structure, structural relaxation and ion diffusion in sodium disilicate melts. Eur. Lett. 59, 708–713.

Mysen, B.O., 1988. Structure and Properties of Silicate Melts. Elsevier, Amsterdam. 354 pp.

Myuller, R.L., 1955. A valence theory of viscosity and fluidity for high-melting glass-forming materials in the critical temperature range. Zh. Prikl. Khim. 28, 1077–1087.

Neuville, D.R., Courtial, P., Dingwell, D.B., Richet, P., 1993. Thermodynamic and rheological properties of rhyolite and andesite melts. Contrib. Mineral. Petrol. 113, 572–581.

Ohlhorst, S., Behrens, Holtz, F., 2001. Compositional dependence of molar absorptivities of near-infrared OH- and H_2O bands in rhyolitic to basaltic glasses. Chem. Geol. 174, 5–20.

Persikov, E.S., 1991. The viscosity of magmatic liquids: experiment generalized patterns, a model for calculation and prediction, applications. In: Perchuk, L.L., Kushiro, I. (Eds.), Physical Chemistry of Magmas, Advances in Physical Chemistry. Springer, Berlin, pp. 1–40.

Poggemann, J.F., Heide, G., Frischat, G.H., 2003. Direct view of the structure of different glass fracture surfaces by atomic force microscopy. J. Non-Cryst. Solids 326/327, 15–20.

Richet, P., 1984. Viscosity and configurational entropy of silicate melts. Geochim. Cosmochim. Acta 48, 471–483.

Richet, P., Bottinga, Y., 1995. Rheology and configurational entropy of silicate melts. In: Stebbins, J., McMillan, P.F., Dingwell, D.B. (Eds.), Structure, Dynamics and Properties of Silicate Melts. Reviews in Mineralogy, vol. 32. Mineralogical Society of America, Washington, DC, pp. 21–66.

Richet, P., Lejeune, A.M., Holtz, F., Roux, J., 1996. Water and the viscosity of andesite melts. Chem. Geol. 128, 185–197.

Russell, J.K., Giordano, D., 2005. A model for silicate melt viscosity in the System $MgSi_2O_6$–$CaAl_2Si_2O_8$–$NaAlSi_3O_8$. Geochim. Cosmochim. Acta. 69, 5333–5349.

Russell, J.K., Giordano, D., Dingwell, D.B., Hess, K.U., 2002. Modelling the non-Arrhenian rheology of silicate melts: numerical considerations. Eur. J. Mineral. 14, 417–427.

Russell, J.K., Giordano, D., Dingwell, D.B., 2003. High-temperature limits on viscosity of non-Arrhenian silicate melts. Am. Mineral. 88, 1390–1394.

Shaw, H.R., 1972. Viscosities of magmatic silicate liquids: an empirical model of prediction. Am. J. Sci. 272, 438–475.

Tammann, G., Hesse, W., 1926. Die Abhängigkeit der Viskosität von der Temperatur bei unterkühlten Flüssigkeiten. Z. Anorg. Allg. Chem. 156, 245–257.

Toplis, M.J., Dingwell, D.B., Hess, K.U., Lenci, T., 1997. Viscosity, fragility and configurational entropy of melts along the join SiO_2–$NaAlSiO_4$. Am. Mineral. 82, 979–990.

Vogel, D.H., 1921. Temperaturabhängigkeitsgesetz der Viskosität von Flüssigkeiten. Phys. Z. 22, 645–646.

Webb, S.L., Müller, E., Büttner, H., 2004. Anomalous rheology of peraluminous melts. Am. Mineral. 89, 812–818.

Whittington, A., Richet, P., Linard, Y., Holtz, F., 2000. Water and the viscosity of depolymerised aluminosilicate melts. Geochim. Cosmochim. Acta 64, 3725–3736.

Whittington, A., Richet, P., Linard, Y., Holtz, F., 2001. The viscosity of hydrous phonolites and trachytes. Chem. Geol. 174, 209–223.